

Origin of the time-dependence of wet oxidation of AlGaAs

Carol I.H. Ashby, Monica M. Bridges, Andrew A. Allerman, B.E. Hammons,
and Hong Q Hou

Sandia National Laboratories, Albuquerque, NM 87185-0603

(Received

The time-dependence of the wet oxidation of high-Al-content AlGaAs can be either linear, indicating reaction-rate limitation, or parabolic, indicating diffusion-limited rates. The transition from linear to parabolic time dependence can be explained by the increased rate of the formation of intermediate As_2O_3 vs. its reduction to elemental As. A steadily increasing thickness of the As_2O_3 -containing region at the oxidation front will shift the process from the linear to the parabolic regime. This shift from reaction-rate-limited (linear) to diffusion-limited (parabolic) time dependence is favored by increasing temperature or increasing Al mole fraction.

Rapid oxidation of AlGaAs with a high aluminum mole fraction (>85% Al) using water entrained in an inert gas such as N_2 or Ar [1] is an enabling technology for high-efficiency vertical cavity surface emitting lasers (VCSELs) with wall-plug efficiencies >50% [2]. Wet oxidation has also been employed for gallium-arsenide-on-insulator (GOI) metal semiconductor field effect transistors (MESFETs) [3] and metal-insulator-semiconductor field effect transistors (MISFETs) [4]. For device fabrication, a linear relationship between oxidation time and oxidized depth is highly desirable for precise control of device characteristics. However, the time-dependence of oxidation has been reported to vary between linear (reaction-rate-limited) and parabolic (diffusion limited) [5-9]. We present here an explanation for these observations that should permit selection of suitable reaction conditions to promote linear oxidation for more reproducible device characteristics.

The AlGaAs layers of the laterally oxidized samples were first exposed by etching a mesa structure. Lateral oxidations were performed between 400 and 440 °C with 80 ± 0.5 °C water and a flow rate of 3.0 slm through a 4"-diam, 3-zone tube furnace. Oxidation depths were measured using scanning electron microscopy (SEM).

The Raman spectra presented here employed planar 2- μm -thick $\text{Al}_{0.98}\text{Ga}_{0.02}\text{As}$ layers on GaAs that were oxidized from the surface down rather than laterally from an exposed edge [10]. Prior to wet oxidation, a 300-Å GaAs cap was selectively removed using a citric acid/peroxide mix [5:1 of (1g citric monohydrate/1g H_2O):30% H_2O_2]. Samples were heated to the reaction temperature (400 < T < 455 °C) in dry nitrogen. The nitrogen flow (0.4 slm, 2-in. diam. tube) was then switched to bubble through 80 ± 1 °C water. The reaction was terminated by switching to a dry nitrogen flow. Raman spectra were measured in the $x(y',y'+z')\bar{x}$ backscattering configuration (y' and z' parallel to (110) planes) using 514.5-nm light at < 85 W/cm².

To first order, oxidation rates are determined by the Al mole fraction in the oxidizing layer [6]. However, the time dependence of the reaction rate for samples with

identical Al mole fraction has been observed to vary depending on individual processing conditions. Many workers operate in a reaction-rate-limited regime (linear time dependence) to facilitate more precise control of oxidized depth in device structures and others report diffusion-limited behavior (parabolic time dependence). Extrapolations of oxidized depth vs. time curves often fail to pass through the origin, with deviations in both directions having been reported. This complicates mechanistic interpretations. However, sufficient information is available about the temperature and composition dependence of wet oxidation rates to support the following understanding of the important dynamic characteristics that determine the time dependence.

The Deal and Grove model for oxidation [11] describes the temporal dependence of an oxidation process as the sum of a linear and a parabolic term,

$$\frac{d^2}{k_{\text{diff}}} + \frac{d}{k_{\text{rxn}}} = t \quad (1),$$

where the linear term dominates when the oxidation rate is reaction-rate limited and the parabolic term dominates when the rate is diffusion limited. A range of dependences on time have been reported for wet oxidation of AlGaAs. The oxidation of the most preferred device composition of $\text{Al}_{0.98}\text{Ga}_{0.02}\text{As}$ is generally reported to be linear from 380 to 440 °C [6], while the oxidation of AlAs has been reported to have a parabolic dependence from 370 to 450 °C [7]. Another study of AlAs has reported a linear time dependence at 356 °C, a parabolic dependence at 516 °C, and a mixed linear/parabolic dependence at intermediate temperatures [8]. Yet another study of AlAs has shown linear dependence at T ≤ 350 °C and parabolic behavior at T ≥ 375 °C [9].

To explain why a shift occurs between reaction-rate-limited and diffusion-limited regimes, it is necessary to have an understanding of the chemical nature of the reaction. Raman spectra of partially oxidized planar AlGaAs structures (Fig. 1) always

DISCLAIMER

This report was prepared as an account of work sponsored by an agency of the United States Government. Neither the United States Government nor any agency thereof, nor any of their employees, make any warranty, express or implied, or assumes any legal liability or responsibility for the accuracy, completeness, or usefulness of any information, apparatus, product, or process disclosed, or represents that its use would not infringe privately owned rights. Reference herein to any specific commercial product, process, or service by trade name, trademark, manufacturer, or otherwise does not necessarily constitute or imply its endorsement, recommendation, or favoring by the United States Government or any agency thereof. The views and opinions of authors expressed herein do not necessarily state or reflect those of the United States Government or any agency thereof.

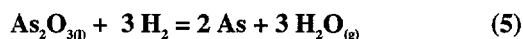
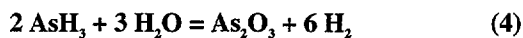
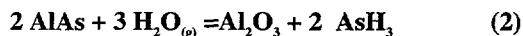
DISCLAIMER

Portions of this document may be illegible in electronic image products. Images are produced from the best available original document.

reveal a significant amount of elemental As that has been liberated during the oxidation process. These spectra are dominated by crystalline elemental As peaks at 198 and 257 cm^{-1} and a broad feature between 200 and 250 cm^{-1} peaking near 227 cm^{-1} due to amorphous As [12]. At higher reaction temperatures, the broad feature centered at 475 cm^{-1} due to amorphous $\alpha\text{-As}_2\text{O}_3$ is observed [13]. This species, if present, is below the Raman detection level for oxidations performed at 400 and 425 $^\circ\text{C}$ (Fig 1a), but it is present at relatively constant levels throughout the oxidation at 450 $^\circ\text{C}$ (Fig. 1b and 1c). As the oxidation front advances into AlAs or AlGaAs films, one observes relatively constant Raman intensities from As and $\alpha\text{-As}_2\text{O}_3$, while the intensity of the AlAs-like phonon steadily decreases as the AlGaAs is converted to oxide [14]. The constant As intensity indicates continual loss of As to leave the porous Al_2O_3 layer that is essential for rapid oxidation to occur.

Due to the strong ability of low-oxidation state Al to donate electrons to other atoms, H^+ from water can serve as the oxidizing agent for the reaction. In the process, H^+ becomes zero-valent H^0 and can serve as a reducing agent for another species. The importance of H^0 and the presence of both As and As_2O_3 as intermediates in the wet oxidation process can be explained as follows.

Water has been shown to adsorb dissociatively on AlAs at 100 K under UHV conditions to produce Al-O, Al-OH, and As-H type species on the AlAs surface [15]. Since literature values for the thermodynamic quantities of these surface species are unavailable, we have chosen to employ the molecular analogs [16], leading to the initial reaction products described by Eqn. 2



At 425 $^\circ\text{C}$, further reaction of As-H can decompose directly to give As and H_2 , as suggested by the Raman spectra (Eqn 3). As-H can also react with water to produce As_2O_3 , but the free energy change is quite small (Eqn. 4). Given the low-temperature UHV results, it is likely that the observed As_2O_3 results from the combination of reactions like Eqns 2 and 4. Both AsH_3 and As_2O_3 can be readily converted to elemental As for removal from the reacting layer (Eqns. 3 and 5), finally resulting in a porous Al_2O_3 layer, as described by Eqn. 6. Gibbs free energies for Eqns 2-6 at 425 $^\circ\text{C}$ are -451, -153, -22, -131-, and -604 kJ/mole, respectively.

The relationship between the rate of formation and conversion of As_2O_3 to As (Eqns. 4 and 5) and the rate of loss of As from the oxidized layer to leave behind a relatively As-free, porous AlO_x matrix will determine the time dependence of the oxidation rate (Fig. 2). The existence of a thin, dense, amorphous region of a few

nanometers thickness has been observed at the oxidation front of a sample oxidized at 440 $^\circ\text{C}$ by transmission electron microscopy (TEM) [17]. Behind this dense region is a less dense region of amorphous Al_2O_3 that extends back to the exposed mesa edge. The time-evolution of the thickness of the dense region will determine whether linear or parabolic behavior dominates. When the reduction of As_2O_3 to As (Eqn. 5) is sufficiently fast to balance the rate of formation of As_2O_3 (Eqn 4), a thin layer of dense oxide of relatively constant thickness and consisting primarily of Al_2O_3 and As_2O_3 will be found near the oxidation front as it moves deeper into the layer. For shallow oxidations, this will produce the relatively constant As_2O_3 Raman intensity observed in films that were partially oxidized at 450 $^\circ\text{C}$. Under these conditions, a linear time dependence will appear because the diffusional contribution to the reaction rate does not increase significantly as the front moves deeper into the layer for typical reaction depths and times. For long reaction times, the deviation from linearity will become increasingly apparent. If reaction conditions are changed to preferentially increase the formation of As_2O_3 relative to As loss, a steadily increasing thickness of the dense, As_2O_3 -containing layer will form more quickly and the diffusion-limited parabolic time dependence will become dominant.

The transition from linear to parabolic behavior should be favored by conditions that increase the rate of Eqn. 4 relative to that of Eqn. 5. The greater amounts of As_2O_3 seen in the Raman spectra for oxidation at 450 $^\circ\text{C}$ vs. 425 $^\circ\text{C}$ and the relatively constant As signal under the two conditions (Fig. 4) suggest that higher temperatures preferentially enhance Eqn. 4 vs. Eqn. 5 for $\text{Al}_{0.98}\text{Ga}_{0.02}\text{As}$. The temperature-dependent change in ΔG vs. T for Eqn. 4 and 5 shows the rate of increase in favorability of As_2O_3 formation is greater than that of As_2O_3 reduction to As. Whereas $d(\Delta G)/dT$ for As_2O_3 formation changes from -0.004 to -0.022 kJ/mol-K, becoming increasingly more favorable with increasing temperature, the reduction of As_2O_3 to As decreases in favorability from -0.018 to -0.006 kJ/mol-K between 350 and 550 $^\circ\text{C}$. Although activation energies and prefactors for the two reactions are needed to definitively predict the temperature dependence of these reactions, their relative changes in $d(\Delta G)/dT$ vs. T is consistent with a shift in the balance between Eqns. 4 and 5 to favor As_2O_3 buildup and the transition from predominantly linear to predominantly parabolic with increasing temperature that has been reported for AlAs by several groups [7-9].

The transition from reaction-limited (linear) to diffusion-limited (parabolic) behavior for a particular AlGaAs composition will depend on the relative temperature dependences of Eqn. 2-5 as Ga is substituted for Al. Experimental results suggest that Eqn. 4 becomes increasingly important for higher Al contents and higher reaction temperatures, both of which increase total oxidation rates. Replacing Al with Ga in $\text{Al}_x\text{Ga}_{1-x}\text{As}$ will affect the favorability of Eqn. 2 and 6, since ΔG^{698} for Eqn 2 for GaAs is +32 kJ/mol, and may thereby retard wet oxidation as Ga content increases. In

contrast, Eqns. 3-5 do not explicitly include either Al or Ga. Consequently, the reduction of As_2O_3 to As should be relatively independent of the Al/Ga ratio. One would, therefore, expect that there might be a change in the time dependence of the total wet oxidation reaction when the rates for Eqn. 2 is increased or decreased faster than the rates for Eqn. 3-5. For example, the slower rate of Eqn. 2 for higher Ga-content AlGaAs could produce linear behavior under some conditions that produce parabolic behavior for higher Al-content material. This has, in fact, been observed during oxidation of a structure containing 45-nm layers of both 98% and 94% AlGaAs oxidized at 440 °C (Fig. 3). In contrast, the slower rates of formation of As_2O_3 from both compositions at 400 °C permits the reduction and loss of As to keep pace with the oxidation process, and linear behavior is observed for both compositions. The transition from reaction-limited to diffusion limited for these samples lies between 0.2 and 1.3 $\mu\text{m}/\text{min}$ oxidation under our reaction conditions. AlAs shifts from linear toward parabolic between 350 and 375°C, as might be expected from its much faster oxidation rate.

In summary, wet oxidation of high-Al-content AlGaAs produces both elemental As and As_2O_3 as important products that can remain near the reaction front. The thickness of the As_2O_3 -containing region at the oxide/semiconductor interface will determine the time-dependence of the process. A shift from reaction-rate-limited (linear) to diffusion-limited (parabolic) time dependence is favored by increasing temperature or increasing Al mole fraction.

Sandia is a multiprogram laboratory operated by Sandia Corporation, a Lockheed Martin Company, for the United States Department of Energy under Contract DE-AC04-94AL85000.

1. J. M. Dallesasse, N. Holonyak, Jr., A. R. Sugg, T. A. Richard, and N. El-Zein, *Appl. Phys. Lett.* **57**, 2844 (1990).
2. K.L. Lear, J.D. Choquette, R.P. Schneider, Jr., S.P. Kilcoyne, and K. M. Geib, *Electron. Lett.* **31**, 208 (1995).
3. P.A. Parikh, P. M. Chavarkar, and U.K. Mishra, *IEEE Electron. Device Lett.* **18**, 111 (1997).
4. E.I.Chen, N.Holonyak, Jr., and S.A. Maranowski, *Appl. Phys. Lett.* **66**, 2688, (1995).
5. F.A. Kish, S.J. Caracci, N. Holonyak, Jr., K.C. Hsieh, J.E. Baker, S. A. Maranowski, A.R. Sugg, J.M. Dallesasse, R.M. Fletcher, C.P. Kuo, T.D. Osenowski, and M.G. Craford, *J. Electron. Mater.* **21**, 1133 (1992).
6. K. D. Choquette, K. M. Geib, C. I. H. Ashby, R. D. Twesten, O. Blum, H. Q. Hou, D. M. Follstaedt, B. E. Hammons, D. Matthes, and R. Hull, *IEEE J. Select. Topics in Quant. Electron.* **3**, 916 (1997).
7. T. Langenfelder, St. Schröder, and H. Grothe, *J. Appl.Phys.* **82**, 3548 (1997).
8. M. Ochiai, G. E. Giudice, H. Temkin, J. W. Scott, and T. M. Cockerill, *Appl. Phys. Lett.* **68**, 1898 (1996).
9. S. A. Feld, J. P. Loehr, R. E. Sherriff, J. Miemeri, and R. Kaspi, *IEEE Photon. Technol. Lett.* **10**, 197 (1998).
10. C. I. H. Ashby, J. P. Sullivan, P.P. Newcomer, N. A. Missert, H. Q. Hou. B. E. Hammons, M. J. Hafich, and A. G. Baca, *Appl. Phys. Lett.* **70**, 2443 (1997).
11. B. E. Deal and A. S. Grove, *J. Appl. Phys.* **36**, 3770 (1965).
12. G.P. Schwartz, B. Schwartz, D. DiStefano, G.J. Gualtieri, and J.E. Griffiths, *Appl. Phys. Lett.* **34**, 205 (1979).
13. G.P. Schwartz, G.J. Gualtieri, J.E. Griffiths, C.D. Thurmond, B. Schwartz, *J. Electrochem. Soc.* **127**, 2488 (1980).
14. C. I. H. Ashby, J. P. Sullivan, K. D. Choquette, K.M. Geib, and H. Q. Hou, *J. Appl. Phys.* **82**, 3134 (1997).
15. W. J. Mitchell, C.-H. Chung, S.I. Yi, E.L. Hu, and W.H. Weinberg, *J. Vac. Sci. Technol.* **B15**, 1182 (1997).
16. Thermochemical data used in calculations found in O. Kubaschewski, C. B. Alcock, P. J. Spencer, "Materials Thermochemistry", Pergamon Press, UK, 1993.
17. R. D. Twesten, D. M. Follstaedt, and K. D. Choquette, "Vercital-Cavity Surface Emitting Lasers, K. D. Choquette and D. G. Deppe, eds., *Proc. SPIE* **3003**, 55 (1997).

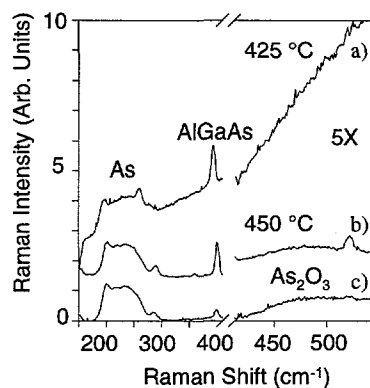


Fig. 1. Time and temperature dependence of the Raman spectra of a 2 μm layer of $\text{Al}_{0.98}\text{Ga}_{0.02}\text{As}$ oxidizing at 425 and 450 °C.

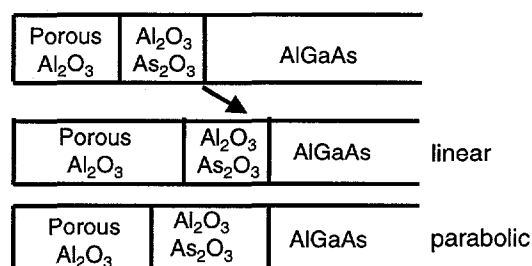


Fig. 2. Increase in rate of As_2O_3 formation relative to its reduction to As and loss to form porous Al_2O_3 shifts rates from linear to parabolic.

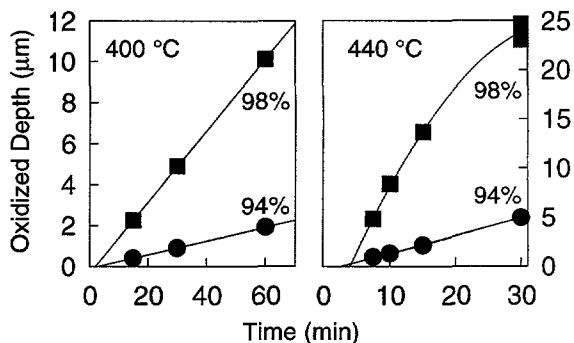


Fig 3: Temperature dependence of oxidation of 45-nm layers of $\text{Al}_{0.98}\text{Ga}_{0.02}\text{As}$ and $\text{Al}_{0.94}\text{Ga}_{0.06}\text{As}$ within the same sample.